https://ntrs.nasa.gov/search.jsp?R=20120012563 2019-08-30T21:12:00+00:00Z

Moisture Fluxes Derived from EOS Aqua Satellite Data for the North Water Polynya over 2003-2009

Linette N. Boisvert

University of Maryland, College Park, Maryland, USA

Thorsten Markus, Claire L. Parkinson

NASA Goddard Space Flight Center, Greenbelt, Maryland, USA

Timo Vihma

Finnish Meteorological Institute, Helsinki, Finland

Abstract

Satellite data were applied to calculate the moisture flux from the North Water polynya during a series of events spanning 2003-2009. The fluxes were calculated using bulk aerodynamic formulas with the stability effects according to the Monin-Obukhov similarity theory. Input parameters were taken from three sources: air relative humidity, air temperature, and surface temperature from the Atmospheric Infrared Sounder (AIRS) onboard NASA's Earth Observing System (EOS) Aqua satellite, sea ice concentration from the Advanced Microwave Scanning Radiometer (AMSR-E, also onboard Aqua), and wind speed from the ECMWF ERA-Interim reanalysis. Our results show the progression of the moisture fluxes from the polynya during each event, as well as their atmospheric effects after the polynya has closed up. These results were compared to results from studies on other polynyas, and fall within one standard deviation of the moisture flux estimates from these studies. Although the estimated moisture fluxes over the entire study region from AIRS are smaller in magnitude than ERA-Interim, they are more accurate due to improved temperature and relative humidity profiles and ice concentration estimates over the polynya. Error estimates were calculated to be 5.56 $x10^{-3}$ g m^{-2} s^{-1}, only 25% of the total moisture flux, thus suggesting that AIRS and AMSR-E can be used with confidence to study smaller scale features in the Arctic sea ice pack and can capture their atmospheric effects. These findings bode well for larger-scale studies of moisture fluxes over the entire Arctic Ocean and the thinning ice pack.

1. Introduction

Polar regions are likely to experience particularly large changes due to global warming; and variations in the moisture flux from the ocean to the atmosphere may serve

as a good indicator of climate changes, because the moisture flux is strongly affected by openings in the sea ice cover, polynyas and leads, which interact with both the atmosphere and ocean [*Barber et al.,* 2001a]. In turn, the moisture flux can have an influence on the sustainability of the Arctic sea ice pack, because large moisture fluxes can increase the cloud cover and alter the surface energy budget. These changes could potentially cause increased ablation of the sea ice pack. This could create a positive feedback loop where larger areas of open water increase the moisture flux into the atmosphere, increase the amount of clouds, which over most of the year increases the net radiation at the ice surface [*Walsh and Chapman*, 1998], and heats the surface to the melting point. During a short period in summer, however, the cloud radiative forcing is negative [*Intrieri et al*., 2002], i.e. the effect of clouds in reducing the solar shortwave radiation absorbed at the ice surface dominates over their effect of increasing the downward longwave radiation. Hence, some negative feedback processes could be operating as well.

Here, moisture flux is defined as the vertical flux of surface moisture due to atmospheric turbulent transport. It is a function of the difference in specific humidity between the surface and air as well as the factors affecting the intensity of turbulent exchange: wind speed, surface roughness, and thermal stratification [e.g., *Launiainen and Vihma*, 1994]. In winter there is little exchange of moisture between thick sea ice and the atmosphere, because in low temperatures the saturation specific humidity is low and, accordingly, the surface-air difference in specific humidity is always low (independent of the relative humidity). Where a polynya is present, however, the large temperature difference between the water and atmosphere allows for large exchange of moisture.

Moisture fluxes over polynyas are sometimes up to 25 times as large as fluxes over thick ice in the winter [*Launiainen and Vihma*, 1994]. The flux of moisture from the ocean to the atmosphere is an important process, because this moisture enhances fog, plume, and cloud formation above and downwind of the polynya [*Arbetter et al*., 2004]. This warm, moisture-rich air from the polynya cools, condenses, and forms fog layers that can rise tens to hundreds of meters [*Smith et al.,* 1983; *Walter,* 1989].

Mailhot et. al [2002] studied plume cloud formation over a polynya using both aircraft observations and the Canadian Compressible Community Model. In one of their sensitivity studies, they found that when they did not allow for the exchange of moisture between the ocean and atmosphere and thus prevented the enhanced moisture flux from the polynya, the relative humidity did not increase to saturation and clouds did not form. Thus, they concluded that the moisture flux from polynyas plays a crucial role in creating clouds. Polynya induced clouds and plumes can modify the surface radiation budget downwind, increasing the downwelling longwave radiation thus reducing the cooling of the surface by as much as 44% [*Pinto and Curry*, 1995; *Pinto et al*., 1995]. These increases could cause a positive radiative feedback, which could enhance ice melt near polynyas, enhancing the moisture flux, and clouds, which cause greater ice melt [*Minnett & Key*, 2007]. Moisture flux, and thus convection, from polynyas can impact the regional climate with changes in atmospheric and surface energy budgets [*Schnell et al*., 1989].

In recent decades, the Arctic sea ice pack has undergone substantial changes. The ice pack has decreased in extent, thickness and compactness [*Parkinson and Cavalieri,* 2008]. The ice pack has shifted from a predominantly multi-year ice pack to a predominantly first-year ice pack [*Nghiem et al.,* 2007]. The melt season length has

increased, meaning that the sea ice begins melting earlier in the spring and freezing up later in the fall [*Markus et al.,* 2009]. All of these factors work together to reduce the ice thickness and ice concentration. This weakened sea ice pack is not as effective an insulator between the ocean and atmosphere as a thick ice pack would be, allowing for more heat and moisture to be exchanged between the ocean and atmosphere.

Producing large-scale estimates of the moisture flux would be valuable for assessing both the current state of the Arctic and the impact of the changing ice pack on the moisture fluxes. Moisture fluxes are already available from atmospheric model reanalyses, but recent studies have demonstrated that reanalyses suffer from serious errors in moisture variables. For example, Cullather *et al*. [2000] showed that in the NCEP/NCAR and NCEP/DOE reanalyses the annual net precipitation (precipitation minus evaporation) is about 60% lower than the water vapour flux convergence, although they should be equal. Jakobson and Vihma [2010] demonstrated that the ERA-40 reanalysis of the ECMWF and rawinsonde sounding data disagree on the vertical distribution of moisture transport to the Arctic, and *Lüpkes et al.* [2010] showed that the ERA-Interim reanalysis has a large moist bias in the lowermost 1 km over the Arctic Ocean. Hence, there is a strong need to develop alternative methods to estimate the moisture fluxes at the atmosphere-ocean interface. Satellite data provide the means for this. In this paper, we describe a small-scale, pilot study preparatory to planned large-scale flux calculations over the entire Arctic region. The small-scale study calculates moisture fluxes from the North Water polynya and evaluates the accuracy of the satellite data.

In recent years, there has been an increase in the amount and quality of satellite data available. Yet few studies have utilized these data to study Arctic polynyas. Previous studies have used satellite data simply to infer the size, shape or existence of polynyas [*Markus and Burns*, 1995; *Martin and Cavalieri*, 1989; *Dey et al*., 1979]. Satellite data add a lot to the information obtained by in situ observations because satellite data have extensive spatial and temporal resolution, allowing for the study of locations that have harsh meteorological conditions and/or are inaccessible.

In this paper, we utilize data from sensors on board NASA's Earth Observing System (EOS) Aqua satellite to examine the North Water polynya moisture fluxes. The North Water polynya was chosen for developing and testing the methodology because it is a recurring feature, which allows calculation of moisture fluxes for several years, and because these results can be compared with results from previous studies.

The North Water polynya (Figure 1) forms in northern Baffin Bay in Smith Sound, located between Ellesmere Island on the west and Greenland on the east [*Topham et al.*, 1983]. This is a predominantly latent heat polynya, which forms in response to an ice dam in Smith Sound that blocks ice from moving into Baffin Bay [*Ito and Muller*, 1977]. This ice is continuously forced southward by persistent northerly winds that channel through the steep sided valleys in the sound [*Ito*, 1985] and by southward ocean currents flowing sometimes at a rate as high as 600 km^3 day^{-1} [*Ito,* 1982]. The North Water polynya is also a sensible heat polynya where some oceanic upwelling results in some ice melt and thinner ice [*Morales Mequeda et al.,* 2004]. This polynya has ice concentrations of 60-80% in the winter months, with the ice being young, thin and thin/medium first-year ice [*Barber et al.,* 2001a; *Gloersen et al.,* 1992]. These features,

along with synoptic conditions, cause the North Water polynya to open and close in a rhythmic fashion for all but the summer months when the region is ice-free [*Morales Maqueda et al.,* 2004]. The southern extent, and thus the overall size of this polynya, changes with each event due to variable weather conditions [*Stirling*, 1980]. *Barber et al.* [2001b] examined the North Water polynya for the period 1979-1996 and found that the frequency of the polynya events increased over that period with the continued reduction in the central Arctic ice coverage. The North Water polynya is an ideal location to study the moisture flux because there has been evidence of large turbulent exchanges at least an order of magnitude larger than the exchange over the sea ice [*Maykut,* 1978] and there is often a downwind fetch that can exceed 100km [*Smith et al.*, 1990].

2. Data

We utilize data from sensors on board NASA's Earth Observing System (EOS) Aqua satellite to examine the North Water polynya moisture fluxes. Aqua was launched on May 4, 2002, and continues to operate. Aqua carries six Earth-observing instruments that collect a wide variety of global data [*Parkinson,* 2003]. It has a near-polar low-Earth orbit with a period of 98.8 minutes and equatorial crossing times of 1:30 a.m. and 1:30 p.m. Specifically, we use data from the Japan Aerospace Exploration Agency (JAXA)'s Advanced Microwave Scanning Radiometer for EOS (AMSR-E) for ice concentration fields and data from NASA's Atmospheric Infrared Sounder (AIRS) for temperature and relative humidity fields.

AIRS is a cross-track scanner collecting data with a 13.5 km spatial resolution in the horizontal and 1 km resolution in the vertical. It has 2378 infrared channels and four visible/near infrared channels, which obtain highly accurate temperature and humidity

profiles and many other physical products dealing with the Earth and its atmosphere. From AIRS we use surface skin temperature of the sea ice, the air temperature at 1000 hPa pressure level, and relative humidity at 1000 hPa level. We use the geopotential heights from AIRS in order to determine the actual heights of the 1000 hPa level. All standard temperature and relative humidity products are level quantities, which means that the values are reported at fixed pressure levels [*Fishbein et al.,* 2011]. The vertical resolution does not vary with elevation because the temperature and humidity profiles are obtained from a 100 level support product temperature or humidity profile using interpolation that is linear to the logarithm of the support pressure [*Susskind and Blaisdell,* 2010]. These values are used in the calculation of the moisture flux and are Level 3 mean daily gridded products covering a 24-hour period for the ascending (equatorial crossing south to north at 1:30 p.m. local time) portion of the orbit [*Aumann et al.,* 2003]. In the polar regions, Aqua makes multiple passes over the study area each day, allowing for daily averages to be produced. These parameters are mapped onto a 1° x 1° global grid.

AMSR-E is a conically scanning global passive microwave radiometer that has 12 channels, with horizontal and vertical polarizations for each of six frequencies, and a spatial resolution ranging from 5.4 to 56 km depending on frequency. On October 4, 2011 AMSR-E stopped functioning after over nine years of successful operations; there are plans to turn it back on in early 2012, in the hopes that it will be able to obtain useful data. The sea ice concentration is created by the NASA Team (NT2) algorithm [*Markus and Cavalieri,* 2000]. The sea ice concentration is defined as the percentage of a pixel

that is covered by sea ice, and the concentration values are mapped onto a 25 km by 25 km polar stereographic grid of the Arctic.

The AMSR-E wind speeds are not available over polynyas and hence are not useful for this study. As a result, 10-m wind speeds were obtained from European Centre for Medium-Range Weather Forecasts (ECMWF) ERA-Interim reanalysis instead (http://data-portal.ecmwf.int/data/d/interim_daily/). The reanalysis combines a first-guess field (based on a 6-hour forecast) as well as in-situ and remote sensing data into an assimilated data set using the 4D-VAR method [*Dee et al*., 2011]. Wind speed data are provided at 6-hour time intervals with a 0.73° by 0.73° spatial resolution.

These data sets were all transposed onto a 25 km by 25 km polar stereographic grid in order to simplify the calculation and comparison of the North Water polynya and its moisture flux. Calculations at 25 km resolution indeed require interpolation of AIRS and wind speed data in north-south direction (in east-west direction, 1° longitude is close to 25 km in our study area). A horizontal resolution equal to that of the sea ice concentration data is, however, essential for the moisture flux calculations, because the spatial variations of the moisture flux are mostly controlled by spatial variations of the surface temperature (which depends above all on the state of the surface: sea ice or open water). The air moisture and wind speed have weaker spatial gradients [e.g. *Tisler et al*., 2008].

3. Methodology

Moisture flux, E, is calculated using the bulk aerodynamic method of *Launiainen and Vihma* [1990],

$$E = \rho C_E (q_s - q_a) V_{10m} \quad (1)$$

where ρ is the air density, C_E is the water vapor transfer coefficient, q_s is the saturation specific humidity at the ice/polynya surface, q_a is air specific humidity at 1000 hPa pressure level, and V_{10m} is the wind speed at 10 m. q_a is calculated on the basis of air temperature and relative humidity. The iterative calculation method [*Launiainen and Vihma*, 1990] allows for variables to have different observation heights above the surface. Taking into account the stability and roughness effects on the vertical profiles, the air temperature, relative humidity and wind speed are all stratified onto a reference height where the calculations are made. The AIRS data include information on the height of the 1000 hPa pressure level, i.e., the observation height of the air temperature and relative humidity. Depending on the surface pressure, however, the height of the 1000 hPa level varies. For example, if the surface pressure is 1010 hPa, the 1000 hPa level locates at the height of approximately 80 m. Then there are cases with the surface pressure less than 1000 hPa, i.e. the 1000 hPa level does not exist in the atmosphere. In these cases we use the standard observation height of 2 m for the relative humidity and air temperature.

The water vapor transfer coefficient over water and ice is calculated based on the Monin-Obukhov similarity theory. Specifically, the measuring height, the roughness lengths for water vapor and momentum, and the effects of stability were taken into account to determine C_E. For the stability effect, we applied the empirical formula of *Holtslag and de Bruin* [1988] under stable stratification (i.e., in most cases over sea ice) and that of *Högström* [1988] under unstable stratification (over polynya). The air specific humidity was calculated on the basis of the observed air temperature and relative

humidity, and the saturation specific humidity at the ice/polynya surface was calculated on the basis of the observed surface skin temperature. The calculation method as a whole is described in detail in *Launiainen and Vihma* [1990].

Since the North Water Polynya fluctuates throughout January and February, we chose the largest polynya each year, 2003-2009, and selected an 11-day period for each polynya event, starting with a day in which the polynya was either not present or had an ice concentration larger than 85%. In each case, the 11-day period ended with the polynya in the process of closing up or having an ice concentration larger than 85% (Table 1 and Figure 2). The moisture flux was calculated for each day during the polynya event.

4. Results

As expected, the calculated moisture fluxes over the solid ice pack were much lower than over the polynya (Figure 2). For example, the moisture flux over the solid ice before the 2003 polynya event was 4.63×10^{-4} g m^{-2} s^{-1} as opposed to 3.01×10^{-2} g m^{-2} s^{-1} over the polynya, which is almost seventy times larger. During the polynya event, the moisture from the polynya is transported over the ice via winds. Once the polynya has closed up, the moisture over the ice remains noticeably larger than before the polynya event. Thus the polynya altered the amount of moisture over the ice pack.

During the 2003 polynya event, which in many respects appears typical, the moisture flux starts out low (day 1) due to the solid ice pack; then once the polynya opens, the moisture flux begins to increase (days 2-3) (Figure 3). When the polynya reaches its largest size, the moisture flux is at its maximum and the moisture is transported via north winds into the Baffin Bay (day 4). These effects are seen for the

next few days, with the maximum moisture flux area becoming smaller (days 5-7). As the polynya begins to close up, the moisture flux decreases over the entire region and the moisture flux from the polynya itself is reduced (days 8-11). Although each polynya event is unique, this sequence is roughly the same in each case. The amount of moisture transferred from the polynya to the atmosphere depends strongly on the ice concentration during the event; the less ice coverage, the larger the moisture flux for all years except 2005. The moisture flux is also dependent on the area of the polynya, which is defined as the enclosed area with ice concentration less than 85%. In most cases, the larger the size of the polynya the larger the flux of moisture. However, the 2007 North Water polynya had the largest area at 33,350 km^2, but did not have the largest moisture flux, with 7.95 x 10^8 g s^{-1}. The 2003 polynya had an area only 80% of that in 2007, but the moisture flux was 2.30 x10^6 g s^{-1} greater than in 2007 (Table 1). The moisture flux depends on the ice concentration as well as on the area, and on the air temperature and moisture and the wind speed. There is also the issue of how the North Water Polynya is formed. Normally, it forms via northerly winds that channel through the Smith Sound, southward ocean currents, and oceanic upwelling. The winds and currents force the ice away from the ice bridge and upwelling helps to sustain lower ice concentrations [*Morales Mequeda et al.,* 2004]. Variations in these factors, for example an increase in the winds and a decrease in the upwelling, could create a smaller polynya with a larger moisture flux, like that seen in 2006.

For each polynya event a transect from the northeast to the southwest through the polynya was studied to understand how the moisture flux progressed over time (Figure 4). The transect, the white line in Figure 1, begins from Greenland in the northeast and

ends near Baffin Island in the southwest. The polynya begins to form and opens up right along the coast in this particular case. This transect was chosen because it passes through the longest fetch of the polynya. On February 9, 2006, the polynya was not present and the moisture flux was very low and uniform, only losing 5.56 x 10^{-3} g m^{-1} s^{-1} as integrated over the entire transect (Figure 4). Once the ice pack began to break up on February 10th and 11th there was a dramatic increase in the amount of moisture exchanged (1.14 x 10^{-1} and 9.53 x 10^{-2} g m^{-1} s^{-1} integrated over the entire transect), and the moisture flux was increased over the ice pack. On February 15-16, the polynya was at its largest area and the integrated moisture flux over the entire transect reached 6.29 x 10^{-1} g m^{-1} s^{-1}. During these days there was a larger flux of moisture over the sea ice. From February 10 to February16 the peak of the moisture flux curve moved along the transect from the northeast to the southwest towards the thick ice pack. The polynya closed up rapidly over the course of a day, and by February 17 and 18 the moisture flux had decreased significantly, down to 7.66 x 10^{-2} g m^{-1} s^{-1} integrated over the transect. Before the polynya opened up there was relatively no flux of moisture between the surface and the atmosphere due to the insulating sea ice, but once the polynya opened up, a large exchange of moisture from the ocean to the atmosphere occurred (Figures 4 and 5).

Although only one example is shown here, each polynya event behaves qualitatively similarly to the 2006 event, although with different flux magnitudes. The total moisture flux from the polynya, integrated over the transect and the duration of the polynya event, ranged from a low value of 4.60 x 10^{-1} g m^{-1} in 2005 (light blue line in Figure 6) to a high value of 3.01 g m^{-1} in 2007 (orange line in Figure 6). The reasons for these differences include differences in the wind speed and air specific humidity as well

as in the size and duration of the polynya event. For the entire polynya, the moisture flux was the greatest out of all the years in 2006 and the smallest in 2005.

The integrated moisture flux over the transect had a qualitatively similar pattern for each polynya event (Figure 6). At the beginning of each event, the integrated moisture flux along the transect is low, averaging 4.46 x 10^{-2} g m^{-1} s^{-1}. The integrated moisture flux over the transect increases as the polynya opens, with its maximum value averaging 4.26 x 10^{-1} g m^{-1} s^{-1} over the different polynya events. After reaching its maximum, the integrated moisture flux over the transect either drops off gradually or sharply, depending on the year, until the last day of the event, when the average integrated moisture flux decreases to 8.37 x 10^{-2} g m^{-1} s^{-1}. Differences arise from year to year depending on how long the moisture flux remains elevated. For instance, in 2003 (black line in Figure 6), the integrated moisture flux remained high from day 1 to day 5, whereas in 2008 (red line in Figure 6) it only remained elevated on days 3-5. The polynya in 2006 behaved differently from the other years because it reached its maximum at day 8 and then dropped off gradually, whereas in the other years the maximum occurred around day 4 and the drop off was more gradual.

5. Error estimates

Errors in the moisture flux calculations arise from uncertainties in the input parameters, specifically the surface temperature, air temperature, relative humidity, wind speed and geopotential height. The surface and air temperature data sets from AIRS include error estimates [*Susskind and Blaisdell,* 2010], which we applied to calculate the average moisture flux errors for each polynya event. The AIRS error estimates are based on 16 different internal convergence tests, the values of which are multiplied by a matrix

that differs for non-frozen ocean and land/ice cases. The coefficients for these matrixes were created using AIRS retrievals and ECMWF 3-hour forecasts on September 24, 2004 [*Susskind and Blaisdell,* 2010]. These average errors were 3.8 K and 3.81 K for the surface and air temperatures, respectively. For the sea surface temperature (SST), however, an error estimate of 0.2 K can be used. The SST of the North Water polynya in winter is always very close to the freezing point because there is no heat source to raise the surface temperature above the freezing point. Instead, the open water surface is strongly losing heat to the atmosphere via sensible and latent heat fluxes and negative net radiation. The relative humidity data set from AIRS did not include any error estimate, but the relative humidity data have been shown to have a 20% error [*Tobin et al.,* 2006, *Gettelman et al.,* 2006]. The relative humidity uncertainty estimates are representative of this region. *Tobin et al*. [2006] used humidity profiles taken from three Atmospheric Radiation Measurement (ARM) program sites that Aqua overflew. One of these sites was in North Slope of Barrow, Alaska; although the site is not on the sea ice, it is along the coast of the Arctic Ocean. The average geopotential height error was 4.5 m. Estimating uncertainties for the ECMWF wind speed has proven challenging because errors have not been accurately determined for this season for the Arctic. *Lüpkes et al.* [2010] estimated uncertainties of 0.6 m/s for the wind speeds in summer, so we applied that value for this study. The accuracy of the water vapor transfer coefficient C_E over the open sea is probably no better than ±20% [*Cronin et al*., 2006]. Average values of the calculated sensitivities, estimated uncertainties, and the final uncertainties for all of the North Water polynya events are shown in Table 2. We assumed that the variables were uncorrelated and this allowed us to make an error estimate by using

$$\sigma_E^2 = \Sigma\ \sigma_x^2\ (dE/dx)^2 \qquad (2)$$

AIRS temperature and humidity profiles are created from different wavelengths. The temperature profile uses channels in the CO_2 Q branch, which occurs at 667 cm^{-1} because it is sensitive to temperature variations at altitudes up to 1 hPa pressure level. 147 channels in this branch are used in the first estimation of the temperature profile. The humidity profile is created using channels on the peaks of some of the strongest absorption features in the 6.7 μm water vapor band. The temperature profile is then updated using 7 out of the 66 channels that the humidity profile uses to produce more accurate estimates [*Susskind et al.,* 2003]. Hence AIRS temperature and humidity are almost independent of each other. Using this method, the uncertainty of the moisture flux, averaged over all polynya events, was calculated to be 5.56 x 10^{-3} g m^{-2} s^{-1}. Compared to the average moisture flux of 2.30 x 10^{-2} g m^{-2} s^{-1}, this amounts to a relative error of 25% only. This is a small error compared to the range of moisture fluxes between the polynya events. The largest uncertainties arise from the large uncertainty of the air temperature, with smaller contributions to the uncertainty coming from the relative humidity, the geopotential height, the surface temperature, and the wind speed.

6. Comparisons

There were no field campaigns during the 2003-2009 study period for the North Water polynya, but during January – June 2008 there was a field campaign and study done of Canada's Cape Bathurst flaw lead polynya region. *Raddatz et al.* [2010] used hourly microwave radiometric profiles of absolute humidity and temperature taken

aboard an icebreaker to study the atmospheric boundary layer. They used these observations to calculate the moisture flux from the surface in the winter, which they classified as January 1 – March 31. During this period they calculated the moisture flux to range from 3.01 x 10^{-4} g m^{-2} s^{-1} to 3.60 x 10^{-3} g m^{-2} s^{-1}. We used AIRS data from January 1 – March 31 for this region to calculate the moisture flux using the same method described previously and we obtained values of 1.46 x 10^{-7} g m^{-2} s^{-1} to 3.66 x 10^{-3} $gm^{-2}s^{-1}$. Their measurements were made at a single point over the polynya, whereas ours were taken from a 25 by 25 km grid, which occasionally also included sea ice. This explains our much smaller minimum moisture flux.. The fact that our calculated maximum values fit so well with those from *Raddatz et al.* [2010] is very encouraging.

We further compared our results with those from the 0.73° by 0.73° ECMWF ERA-Interim full resolution reanalysis data sets for the January 2003 event (http://data-portal.ecmwf.int/data/d/interim_full_daily/). AIRS humidity data over the open ocean, including polynyas, if large enough to be resolved by the model grid, have been assimilated to ERA-Interim only since April 2003, but only under clear-sky conditions [*Dee et al.,* 2011]. Further, the effect on the analysis is small: the down-weighting of the AIRS data is coupled with the fact that the ERA-Interim humidity analysis is highly constrained by other satellite observing systems [*McNally et al.,* 2006]. The specific humidity for AIRS was compared with the specific humidity from ERA-Interim (Figure 7). These were calculated from AIRS relative humidity and air temperature and from ERA-Interim dew point and air temperatures. The specific humidity of AIRS was larger than that of ERA-Interim on most of the days. Specifically, on days 2-6 Figure 7 shows clearly identifiable differences even quite far from the North Water polynya. Sometimes

the absolute difference is up to 1 g kg^{-1}, which corresponds to a relative difference of about 100%. The average specific humidity over the polynya for AIRS was 0.56 g kg^{-1} and for ERA-Interim was 0.47 g kg^{-1}. The ice concentration from AMSR-E was compared with that of ERA-Interim for the 2003 polynya (Figure 8). Due to its coarse resolution, the ERA-Interim sea ice concentration is less accurate than that of AMSR-E. The ERA-Interim ice concentrations are lower in the vicinity of the North Water polynya on days 4-6, but it appears that this area of lower ice concentration does not fluctuate throughout the event, having an average of 62% ice concentration. The AMSR-E ice concentration for the polynya ranges from 56-77%. This can be seen in Figure 8c where there are large ice concentration differences. The ice concentration is very similar over the thick ice pack, but there are many discrepancies over the polynya. For ERA-Interim, the ice concentration starts out too low, before the polynya is even open and then does not reduce its size in day 8-9 when the polynya is actually much smaller. The polynya produced by ERA-Interim ice concentration data is much larger than what is produced by AMSR-E, which can create problems in computing the moisture flux.

The ERA-Interim data for air temperature, surface temperature, dew point temperature, wind speed and ice concentration are used along with the method described in the text to calculate the moisture flux. Due to problems with the ERA-Interim ice concentration for the North Water polynya, their moisture fluxes have some inaccuracies. This can be seen in Figure 9 where AIRS and ECMWF moisture fluxes are compared for the 2003 polynya. The moisture flux of AIRS follows the normal pattern of the North Water polynya, in which size and moisture fluctuates throughout the event. The moisture flux for ECMWF starts out small, but from day 4 onward the area with a large flux

remains constant and too large, also the maximum values are occasionally too large. The specific humidity was less for ERA-Interim and the erroneous ice concentration causes the moisture flux over the polynya to be an average of 4.90 x 10^{-3} g m^{-2} s^{-1} smaller than that for AIRS. AIRS had an average moisture flux over the polynya that was 16% larger than ERA-Interim, which had an average of 2.52 x 10^{-2} g m^{-2} s^{-1}. When comparing the moisture flux over the entire study region then ERA-Interim does in fact have a larger moisture flux, but this is due to the ice concentration. The moisture flux appears to be more reliable from AIRS because of the more accurate ice concentrations. This supports the idea that the AIRS instrument can accurately capture even smaller features in the Arctic sea ice pack.

Finally, the AIRS moisture flux was compared with the full resolution moisture flux product that is produced by ERA-Interim for the 2003 polynya event (Figure 10). In this figure, the ERA-Interim moisture flux follows the pattern of AIRS more closely than what we produced using the variables from ERA-Interim, but the polynya area is often too large and the magnitude of the moisture flux over the polynya is too small in the ERA-Interim product. The average area of the polynya produced by ERA-Interim is 70% larger than that produced by AMSR-E, owing to the larger moisture flux over the entire study region. The average moisture flux over the polynya produced by ERA-Interim is 1.46 x 10^{-2} g m^{-2} s^{-1}, which is 51% smaller than our AIRS moisture flux over the polynya. The ERA-Interim magnitude is not large enough over the polynya, but over the solid ice pack the moisture fluxes are nearly identical. Possible reasons for these differences are due to the relatively poor quality of ERA-Interim ice concentration over the polynya and differing moisture flux algorithms. However when the average moisture flux over the

entire study area is compared, the ERA-Interim moisture flux product is 11% larger in magnitude than that for AIRS. The average moisture flux over the entire region for ERA-Interim is 4.92 x 10^{-3} g m^{-2} s^{-2} and for AIRS is 4.48 x 10^{-3} g m^{-2} s^{-1}. The reason for this is that the ERA-Interim ice concentration for the polynya is larger in area, creating a larger area of elevated moisture flux.

We also compared our calculated moisture fluxes to results from other studies of polynyas and leads in the Arctic and Antarctic. The moisture flux from each individual polynya event depends on the unique meteorological conditions at the specific time and location, but we expect some general consistency among the observations. Moisture fluxes from 13 studies are listed in Table 3. These 13 studies span the Arctic and Antarctic, leads and polynyas, in situ and model data, and cover years from the 1970's to the 1990's. Values of the moisture fluxes for our study fall within the values from the other studies listed in the table. The 2004 polynya had a very similar computed moisture flux to those from the Weddell Sea [*Launianen and Vihma*, 1994] and the Mertz Island Glacier [*Roberts et al.,* 2001], with 2.74 x 10^{-2} g s^{-1} compared to 2.72 x 10^{-2} g s^{-1}. The Northeast Water Polynya in the *Willmott et al.* [1997] study had an area of 4,200 km^2, which most closely resembled the 2005 North Water Polynya of 5,555 km^2. The comparisons for the magnitude of the moisture fluxes were 4.86 x 10^7 g s^{-1} and 8.04 x 10^7 g s^{-1}, with the Northeast Water Polynya having a significantly smaller moisture flux because measurements were made in April and May where turbulent fluxes are much smaller than in the winter months. *Renfrew et al.* [2002] studied coastal polynyas in the Weddell Sea, having an area of 13,000 km^2, which is roughly the same size as the 2006, 2008 and 2009 North Water Polynyas. Even though the coastal Weddell Sea polynyas are

slightly smaller in size it shows good agreement with our results having 2.60 x 10^8 g s^{-1} compared to our estimates of 4.25 x 10^8 g s^{-1}, 2.14 x 10^8 g s^{-1}, and 2.38 x 10^8 g s^{-1}. The 2003 North Water Polynya is the most comparable to the Mertz Glacier Polynya [*Roberts et al.,* 2001] in size and the fact that both polynyas occurred during the winter months. The 2003 North Water polynya had an area of 26,500 km^2 with a moisture flux of 7.97 x 10^8 g s^{-1} and the Mertz Glacier Polynya had an area of 23,000 km^2 with a moisture flux of 6.26 x 10^8 g s^{-1}. The Mertz Glacier Polynya was only 86% of the size of the 2003 polynya, and lost roughly 78% of the amount of moisture as the 2003 North Water polynya, showing that our estimates are reasonable. The fact that all of our calculated moisture fluxes agree with other moisture fluxes measured or calculated using in situ and model data suggests that the data from AIRS are sufficiently accurate for use in moisture flux calculations.

7. Conclusions

For the first time, the moisture flux has been calculated for the North Water Polynya using instruments onboard the Aqua satellite. One polynya event was chosen for each year 2003-2009, allowing us to examine differences in moisture fluxes between individual events and to have multiple events to include in our error estimates. The moisture flux was calculated using the bulk aerodynamic formulas of *Launiainen and Vihma* [1990]. AIRS and AMSR-E have the ability to detect small-scale features as well as their atmospheric effects, so that they can also be used to study polynyas over large spatial and temporal scales. Using this approach, the moisture flux produced by the polynyas can be studied in detail. Although the examined polynya events differ, the moisture flux behaves in a similar fashion in each of them, beginning with low values,

increasing to its maximum when the polynya reaches its largest area, and decreasing as the polynya closes back up. The moisture flux over the most compact ice is often five times smaller before the polynya opens than after it closes, as a result of the moisture that enters the atmosphere during the polynya's presence.

The uncertainties of our moisture flux estimates are calculated to be only 25%, which is quite encouraging. Comparing our moisture flux calculations with those of *Raddatz et al.* [2010], we had very similar results with a difference of 5.79×10^{-5} g m^{-2} s^{-1} on the upper bound and a difference of 3.01×10^{-4} g m^{-2} s^{-1} on the lower bound during the time period. The AIRS moisture flux is an improvement to the ERA-Interim moisture flux because of the improved accuracy of temperature and humidity profiles from AIRS and the higher resolution of AMSR-E ice concentration, which allows for larger and more accurate moisture flux estimates to be made over the polynya. Comparing our moisture flux estimates to those reported in studies on other polynyas, we find that our fluxes fall within one standard deviation of the average of the other studies.

In future studies we will expand our moisture flux calculations to the entire Arctic, in order to observe larger-scale effects of changing sea ice and atmospheric conditions on moisture fluxes over the period of Aqua satellite observations.

References

Andreas, E. L., C. A. Paulson, R. M. Williams, R. W. Lindsay, and J. A. Businger (1979), The turbulent heat flux from Arctic leads, *Boundary-Layer Meteorology,* 17, 57–91.

Arbetter, T. E., A. H. Lynch, and D. A. Bailey (2004), Relationship between synoptic forcing and polynya formation in the Cosmonaut Sea: 1. Polynya climatology, *J. Geophys. Res*., 109, C04022, doi:10.1029/2003JC001837.

Aumann, H. H, M. T. Chahine, C. Gautier, M. D. Goldbery, E. Kalnay, L. M. McMillin, H. Revercomb, P. W. Rosenkranz, W. L. Smith, D. H. Staelin, L. L. Strow, and J. Susskind (2003), AIRS/AMSU/HSB on the Aqua Mission: Design, Science

Objectives, Data Products, and Processing Systems, *IEEE Transactions on Geoscience and Remote Sensing,* 41, 253-264.

Barber, D. G., R. Marsden, P. Minnett, G. Ingram, and J. Piwowar (2001a), Physical processes within the North Water (NOW) polynya, *Atmos. Ocean,* 39, 163-166.

Barber, D. G., J. M. Hanesiak, W. Chan, and J. Piwowar (2001b), Sea-ice and meteorological conditions in northern Baffin Bay and the North Water polynya between 1979 and 1996, *Atmosphere-Ocean,* 39, 343–359.

Cronin M.F., C. W. Fairall, and M. J. McPhaden (2006), An assessment of buoy derived and numerical weather prediction surface heat fluxes in the tropical Pacific, *J. Geophys. Res.,* 111, C06038, doi:10.1029/2005JC003324.

Cullather R.I., D. H. Bromwich, M. C. Serreze (2000), The atmospheric hydrologic cycle over the Arctic basin from reanalyses. Part I: comparison with observations and previous studies, *Journal of Climate,* **13**: 923–937.

Dee D.P., S. M. Uppala, A. J. Simmons, P. Berrisford, P. Poli, S. Kobayashi , U. Andrae, M. A. Balmaseda, G. Balsamo, P. Bauer, P. Bechtold, A. C. M. Beljaars, L. van de Berg, J. Bidlot, N. Bormann, C. Delsol, R. Dragani, M. Fuentes M, A. J. Geer, L. Haimberger, S. B. Healy, H. Hersbach, E. V. Hólm, L. Isaksen, P. Kållberg, M. Köhler , M. Matricardi, A. P. McNally, B. M. Monge-Sanz, J.-J. Morcrette, B.-K. Park, C. Peubey, P. de Rosnay, C. Tavolato, J.-N. Thepaut, and F. Vitart (2011), The ERA-Interim reanalysis: configuration and performance of the data assimilation system, *Q. J. R. Meteorol. Soc.,* 137, 553–597, doi:10.1002/qj.828.

Fishbein, E., S-Y. Lee, E. Manning, E. Maddy, and W.W. McMillan (2011), AIRS/AMSU/HSB Version 5 Level 2 Product Levels, Layers and Trapezoids, E. T. Olsen (*Eds.),* Jet Propulsion Laboratory, Pasadena, California, USA.

Dey, B., H. Moore, and A. Gregory (1979), Monitoring and mapping sea ice breakup and freeze-up of Arctic Alaska from satellite data, *Arctic and Alpine Research*, 11, 229-242.

Gettelman, A., W. D. Collins, E. J. Fetzer, A. Eldering, F. W. Irion, P. B. Duffy, and G. Bala (2006), Climatology of Upper-Tropospheric Relative Humidity from the Atmospheric Infrared Sounder and Implications for Climate, *J. Climate*, 19, 6,104-6,121.

Gloersen, P., W. J. Campbell, D. J. Cavalieri, J. C. Comiso, C. L. Parkinson, and H. J. Zwally (1992), Arctic and Antarctic sea ice, 1978-1987: Satellite passive-microwave observations and analysis. *NASA Special Publications*, SP-511, 290 pp.

Gultepe, I., G. A. Isaac, A. Williams, D. Marcotte, and K. B. Strawbridge (2003), Turbulent heat fluxes over leads and polynyas, and their effects on Arctic clouds during FIRE.ACE: Aircraft observations for April 1998, *Atmos. Ocean*, 41, 15 – 34.

den Hartog, G., R. J. Smith, D. R. Anderson, D. R. Topham, and R. G. Perkin (1983), An investigation of a polynya in the Canadian Archipelago, 3, Surface heat flux, *J. Geophys. Res.*, 88, 2911-2916.

Högström, U. (1988), Non-dimensional wind and temperature profiles in the atmospheric surface layer: A re-evaluation, *Bound.-Layer Meteorol*., 42, 55–78.

Holtslag, A. A. M., and H. A. R. de Bruin (1988), Applied modeling of the nighttime surface energy balance over land, *J. Appl. Meteorol*., 37, 689– 704.

Intrieri, J., C. W. Fairall, M. D. Shupe, P. O. G. Persson, E. L. Andreas, P. S. Guest, and R. E. Moritz (2002), Annual Cycle of Arctic Surface Cloud Forcing at SHEBA, *J. Geophys. Res*. 107, 8039, doi: 10.1029/2000JC000439.

Ito, H., and F. Muller (1977), Horizontal movement of fast ice in the North Water area, *J. Glaciology*, 19, 547-554.

Ito, H. (1982), Wind through a channel: Surface wind measurements in Smith Sound and Jones Sound in northern Baffin Bay, *J. Applied Meteorology*, 21, 1,053-1,062.

Ito, H. (1985), Decay of the sea ice in the North Water area: Observation of ice cover in Landsat imagery, *J. Geophys. Res*., 90, 8,102-8,110.

Jakobson, E. and T. Vihma (2010), Atmospheric moisture budget over the Arctic on the basis of the ERA-40 reanalysis. *Int. J. Climatol.*, **30**: 2175–2194, DOI: 10.1002/joc.2039.

Kurtz, D. D. and D. H. Bromwich (1985), A recurring, atmospherically forced polynya in Terra Nova Bay. *In* Jacobs, S. S., *ed., Oceanology of the Antarctic continental shelf,* Washington, DC, American Geophysical Union, 177-201. (Antarctic Research Series 43.)

Launiainen, J., and T. Vihma (1990), Derivation of turbulent surface fluxes – An iterative flux-profile method allowing arbitrary observing heights, *Environmental Software*, 5, 113-124.

Launiainen, J., and T. Vihma (1994), On the surface heat fluxes in the Weddell Sea, *The Polar Oceans and Their Role in Shaping the Global Environment*, Nansen Centennial Volume, Geophysical Monogram Series, 85, edited by O.M. Johannessen, R. Muench, and J.E. Overland, pp., 399-419, AGU, Washington, D.C.

Lüpkes, C., T. Vihma, E. Jakobson, G. Konig-Langlo, and A. Tetzlaff (2010), Meteorological observations from ship cruises during summer to the central Arctic: A comparison with reanalysis data, *Geophys. Res. Lett.,* 37, L09810, doi:10.1029/2010GL042724.

Mailhot, J., A. Tremblay, S. Bélair, I. Gultepe, and G. A. Isaac (2002), Mesoscale simulation of surface fluxes and boundary layer clouds associated with a Beaufort Sea polynya, *J. Geophys. Res.,* 107, doi:10.1029/2000JC000429.

Markus, T., and B.A. Burns (1995), A method to estimate subpixel-scale coastal polynyas with satellite passive microwave data, *J. Geophys. Res.,* 100, 4,473–4,487.

Markus, T., and D. J. Cavalieri (2000), An enhancement of the NASA Team sea ice algorithm. *IEEE Transactions on Geoscience and Remote Sensing,* 38, 1,387-1,398.

Markus, T., J. C. Stroeve, and J. Miller (2009), Recent changes in Arctic sea ice melt onset, freezeup, and melt season length, *J. Geophys. Res.,* 114, C12024, doi:10.1029/2009JC005436.

Martin, S., and D. J. Cavalieri (1989), Contributions of the Siberian Shelf polynyas to the Arctic Ocean intermediate and deep water, *J. Geophys. Res.,* 94, 12,725-12,738.

Maykut, G. A. (1978), Energy Exchange Over Yound Sea Ice in the Central Arctic, *J. Geophys Res.*, 83, doi:10.1029/JC083iC07p0646.

McNally A. P., P.D. Watts, J. A. Smith, R. Engelen, G. A. Kelly, J. N. Thepaut and M.

Matricardi (2006), The assimilation of AIRS radiance data at ECMWF, *Q. J. R. Meteorl. Soc.*, 132: 935-957.

Minnett, P. J., and E. L. Key (2007), Meteorology and atmosphere – Surface coupling in and around polynyas, Smith, W.O.J., Barber, D.G. (Eds.), In: *Polynyas: Windows to the World*, Elsevier, Amsterdam.

Morales Maqueda, M. A., A. J. Willmott and N. R. T. Biggs (2004), Polynya Dynamics: A review of observations and modeling, *Rev. Geophys., 42*, RG1004, doi:10.1029/2002RG000116.

Nghiem, S. V., I. G. Rigor, D. K. Perovich, P. Clemente-Colon, J. W. Weatherly, and G. Neumann (2007), Rapid reduction of Arctic perennial sea ice, *Geophys. Res. Lett.,* 34, L19504, doi:10.1029/2007GL031138.

Parkinson, C. L. (2003), Aqua: An Earth-observing satellite mission to examine water and other climate variables, *IEEE Transactions on Geoscience and Remote Sensing,* 41(2), 173-183.

Parkinson, C. L., and D. J. Cavalieri (2008), Arctic sea ice variability and trends, 1979-2006, *J. Geophys. Res.,* 113, C07003, doi:10.1029/2007JC004558.

Pease, C. H. (1987), The size of wind-driven coastal polynyas, *J.Geophys. Res*., 92, 7,049–7,059.

Pinto, J.O., J. A. Curry, and K. L. McInnes (1995), Atmospheric convective plumes emanating from leads 1. Thermodynamic structure, *J. Geophys. Res.,* 100, 4,621-4,631.

Pinto, J. O., and J. A. Curry (1995), Atmospheric convective plumes emanating from leads 2. Microphysical and radiative processes, *J. Geophys. Res.,* 100, 4,633–4,642.

Pinto, J. O., J. A. Curry, A. H. Lynch, and P. O. G.Persson (1999), Modeling clouds and radiation for the November 1997 period of SHEBA using a column climate model, *J. Geophys. Res.,* 104, 6,661 – 6,678.

Pinto, J. O., A. Alam, J. A. Maslanik, J. A. Curry, and R. S. Stone (2003), Surface characteristics and atmospheric footpring of springtime Arctic leads at SHEBA, *J. Geophys. Res.,* 108, doi:10.1029/2000JC000473.

Raddatz, R. L., M. G. Asplin, L. Candlish, and D. G. Barber (2010), General Characteristics of the Atmospheric Boundary Layer Over a Flaw Lead Polynya Region in Winter and Spring, *Boundary-Layer Meteorol.,* 138, 321-335, doi:10.1107/s10546-010-9557-1.

Renfrew, I. A., J. C. King, and T. Markus (2002), Coastal polynyas in the southern Weddell Sea: Variability of the surface energy budget, *J. Geophys. Res*., 107, doi:10.1029/2000JC000720.

Roberts, A., I. Allison, and V. I. Lytle (2001), Sensible- and latent-heat-flux estimates over the Mertz Glacier polynya, East Antarctica, from in-flight measurements, *Annals of Glaciology,* 33, 377-384.

Schnell, R. C., R. G. Barry, M. W. Miles, E. L. Andreas, L. F. Radke, C. A. Brock, M. P. McCormick, and J. L. Moore (1989), Lidar detection of leads in Arctic sea ice, *Letters to Nature*, 339, 530 – 532.

Smith, S. D., R. J. Anderson, G. den Hartog, D. R. Topham, and R. G. Perkin (1983), An investigation of a polynya in the Canadian Archipelago, 2, Structure of turbulence and sensible heat flux, *J. Geophys. Res.,* 88, 2,900-2,910.

Smith, S. D., R. D. Muench, and C. H. Pease (1990), Polynyas and leads: An overview of physical processes and environment, *J. Geophys. Res.,* 95, 9,461–9,479.

Stirling, I. (1980), The biological importance of polynyas in the Canadian Arctic, *Arctic*, 33, 303-315.

Susskind, J., C. D. Barnett, and J. M. Blaisdell (2003), Retrieval of atmospheric and surface parameters from AIRS/AMSU/HSB data in the presence of clouds, *IEEE Trans. Geosci. Remote Sensing,* 41, 390-409.

Susskind, J. and J. Blaisdell (2010), AIRS/AMSU/HSB Version 5 Level 2 Quality Control and Error Estimation, E. T. Olsen (Eds.), Jet Propulsion Laboratory, California, USA.

Tisler, P., T. Vihma, G. Müller, and B. Brümmer (2008), Modelling of warm-air advection over Arctic sea ice, *Tellus,* 60(4), 775-788.

Tobin, D.C., H. E. Revercomb, R. O. Knuteson, B. M. Lesht, L. L. Strow, S. E. Hannon, W. F. Feltz, L. A. Moy, E. J. Fetzer, and T. S. Cress (2006), Atmospheric Radiation Measurement site atmospheric state best estimates for Atmospheric Infrared Sounder temperature and water vapor retrieval validation, *J. Geophys. Res., 111,* D09S14, doi:10.1029/2005JD006103.

Topham, D. R., R. G. Perkin, S. D. Smith, A. J. Anderson, and G. den Hartog (1983), An investigation of a polynya in the Canadian Archipelago, 1, Introduction and oceanography*, J. Geophys. Res.,* 88, 2,888-2,988.

Walsh, J. E. and W. L. Chapman (1998), Arctic cloud-radiation-temperature associations in observational data and atmospheric reanalyses, *J. Climate*, 11, 3,030-3,045.

Walter, B. A. (1989), A study of the planetary boundary layer over the polynya downwind of St. Lawrence Island in the Bering Sea using aircraft data, *Boundary-Layer Meteorology,* 48, 255–282.

Willmott, A. J., M. A. Morales Maqueda, and M. S. Darby (1997), A model for the influence of wind and oceanic currents on the size of a steady-state latent heat coastal polynya. *J. Physical Oceanography*, 27, 2,256 – 2,275.

Table 1. North Water Polynya Events

Year	**2003**	**2004**	**2005**	**2006**	**2007**	**2008**	**2009**	**All Years**
Polynya Dates	1/9-1/19	1/9-1/19	1/9-1/19	2/8-2/18	2/5-2/15	1/18-1/28	1/20-1/30	
Mean Moisture Flux x 10^{-3} (entire box) (g m^{-2} s^{-1})	4.75	3.13	0.58	2.89	4.75	2.20	1.50	2.78
Mean Moisture flux, polynya x 10^{-2} (g m^{-2} s^{-1})	3.01	2.74	1.45	3.19	2.38	1.59	1.74	2.30
Mean of Max Moisture Flux x 10^{-2} (g m^{-2} s^{-1})	4.91	4.81	1.90	4.49	4.44	2.64	2.91	3.73

Mean Polynya Size (km^2)	26500	15170	5555	13625	33350	13465	13693	17338
Correlation between polynya size & mean moisture flux (R)	0.71	0.79	0.48	0.54	0.79	0.71	0.41	
Mean Ice Concentration of polynya (%)	66.24	63.37	71.45	63.55	61.34	69.73	63.37	65.58
Correlation between ice concentration & mean moisture flux (R)	-0.89	-0.86	-0.50	-0.93	-0.74	-0.88	-0.79	

Table 2. Sensitivity of the ocean-atmosphere moisture flux over the polynya to different input uncertainties.

Variable (x)	**$d\rho/dx$**	**σ_x**	**$\sigma_x\, d\rho/dx$**
T_a (K)	2.77×10^{-3}	3.81	1.06×10^{-2}
T_s (K) (65%) *	2.77×10^{-3}	3.80	1.05×10^{-2}
SST (K) (35%) *	2.77×10^{-3}	0.2	5.54×10^{-4}
GH (m)	2.77×10^{-5}	4.45	1.23×10^{-4}
Variable (x)	**dq_s/dx**	**σ_x**	**$\sigma_x\, dq_s/dx$**
T_s (K) (65%)	1.97×10^{-3}	3.80	7.49×10^{-3}
SST (K) (35%)	1.97×10^{-3}	0.2	3.94×10^{-4}
Variable (x)	**dq_a/dx**	**σ_x**	**$\sigma_x\, dq_a/dx$**
T_a (K)	1.75×10^{-3}	3.81	6.67×10^{-3}
RH (%)	2.42×10^{-2}	0.2	4.84×10^{-3}

Variable (x)	**dE/dx**	**σ_x**	**σ_x dE/dx**
ρ ($kg\ m^{-3}$)	1.76×10^{-5}	1.17	2.06×10^{-5}
C_E	2.07×10^{-2}	1.6×10^{-3}	8.28×10^{-6}
U ($m\ s^{-1}$)	5.64×10^{-6}	0.6	3.38×10^{-6}
q_s ($g\ kg^{-1}$)	6.28×10^{-3}	0.52	3.27×10^{-3}
q_a ($g\ kg^{-1}$)	6.28×10^{-3}	0.71	4.46×10^{-3}
σ_E ($g\ m^{-2}\ s^{-1}$)	5.56×10^{-3}		
<E> ($g\ m^{-2}\ s^{-1}$)	2.30×10^{-2}		

*The surface temperature errors use the average ice concentration to utilize the errors of both the surface temperature from AIRS and the SSTs.

Table 3. Comparisons of Moisture Fluxes x 10^{-5} (g m^{-2} s^{-1})

Study	Region, Time of Year, Year	Data Type/Spatial Size	Length or Area	Moisture Flux x 10^{-3} (g m^{-2} s^{-1})
This study, 2011	North Water, Jan/Feb, 2003-2009	AIRS, ECMWF 25km^2	17,338 km^2 (average) 5,555-33,350 km^2	2.30 (average) 1.45– 3.19
Andreas et al., 1979	Leads, Arctic, March/April, 1974	AIDJEX Lead Experiment In situ/point measurement	20 km	2.09
Den Hartog et al., 1983	Dundas Island, Arctic, March, 1980	In situ/point measurement	0.3-0.7 km	2.04
Gultepe et al., 2003	Polynya, Beaufort Sea, April, 1998	FIRE.ACE Experiment, In situ/point measurements, flights over 68-71.5N° lat x 133-139° lon	17-65 km	1.60
Kurtz & Bromwich, 1985	Antarctica, Winter, 1985	In situ/point measurement	1,300 km^2	2.72
Launianen & Vihma, 1994	Weddell Sea, Antarctic, 1990-1992	5 buoys drifting from 50-75°S lat x 0-60°W lon	10^6 km^2	3.19
Pease, 1987	Bering Sea, Arctic, Feb 1982, 83, 85	Airplane flyover, model	10-20 km	3.13
Pinto et al., 1995	Wide Arctic Lead	1-D model, 100m	0.1 km	2.12
Pinto et al., 1999	Arctic Leads, November, 1997	In situ, SHEBA, 80km	N/A	2.00
Pinto et al., 2003	Lead, Beaufort Sea, Late April –Early May, 1998	In situ, SHEBA, 5km	0.4 km	1.20
Renfew et al., 2002	Weddell Sea Polynya, Antarctica, 1992-1998	SSM/I, in situ, NCEP/NCAR, models 6.25km^2	13,000 km^2	2.00
Roberts et al., 2001	Mertz Glacier Polynya, Antarctica, August, 1999	In situ from airborne flights, 30km	23,000 km^2	2.72
Schnell et al., 1989	Lead, Central Arctic	Model	0.05-20 km	1.56 – 2.08
Willmott et al., 1997	Northeast Water Polynya, Arctic, April & May, 1991	Monthly mean climatology, 79.5°N, 12.5°W	4,200 km^2	1.16

Description of Figures

Figure 1. Maps of the Arctic region and the North Water polynya study area. Red signifies land, black is the outline of the coastlines, the white line is the transect line used in this study, and all other colors correspond to sea ice concentration (%). The polynya box shown is 562,500 km^2.

Figure 2. Maps of daily ice concentration [IC] (%) (top row) and moisture flux [MF] (g m^{-2} s^{-1}) (bottom row) for each polynya event. Black is land. All maps cover the same region as the polynya map of Figure 1.

Figure 3. Maps of daily ice concentration [IC] (%) (top row) and moisture flux [MF] (g m^{-2} s^{-1}) (bottom row) for the 2003 North Water polynya event. Black is land. All maps cover the same region as the polynya map of Figure 1.

Figure 4. Transects of the moisture flux (g m^{-2} s^{-1}) for the 2006 polynya event (see white line in Figure 1). Red line signifies moisture flux; blue line signifies ice of ≥ 85% concentration, no line signifies the polynya. The figure shows plots for Days 2-11 of the 2006 polynya event.

Figure 5. Maps of daily ice concentration [IC] (%) (top row) and moisture flux [MF] (g m^{-2} s^{-1}) (bottom row) for the 2006 North Water polynya event. Black is land. All maps cover the same region as the polynya map of Figure 1.

Figure 6. Total integrated moisture flux along the transect for each of the years in this study.

Figure 7. Comparison of AIRS and full resolution ECMWF specific humidity (g kg^{-1}) for the 2003 polynya event. A) AIRS specific humidity, B) ECMWF specific humidity, C) Difference between AIRS specific humidity and ECMWF specific humidity. Land is black.

Figure 8. Comparison of AMSR-E and full resolution ECMWF ice concentration (%) for the 2003 polynya event. A) AMSR-E ice concentration, B) ECMWF ice concentration, D) Difference between AMSR-E and ECMWF ice concentrations. Land is black.

Figure 9. Comparison of AIRS moisture fluxes with full resolution ECMWF moisture fluxes for the 2003 North Water polynya event. A.) Calculated AIRS moisture flux (g m^{-2} s^{-1}), B.) Calculated ECMWF moisture flux (g m^{-2} s^{-1}), C.) Difference between the AIRS and the ECMWF moisture flux (g m^{-2} s^{-1}). Black is land.

Figure 10. Comparison of AIRS moisture fluxes with full resolution ECMWF moisture fluxes for the 2003 North Water polynya event. A.) Calculated AIRS moisture flux (g m^{-2} s^{-1}) using the Monin-Obukhov similarity theory, B.) ECMWF moisture flux (g m^{-2} s^{-1}), C.) Difference between the AIRS and the ECMWF moisture flux (g m^{-2} s^{-1}). Black is land.

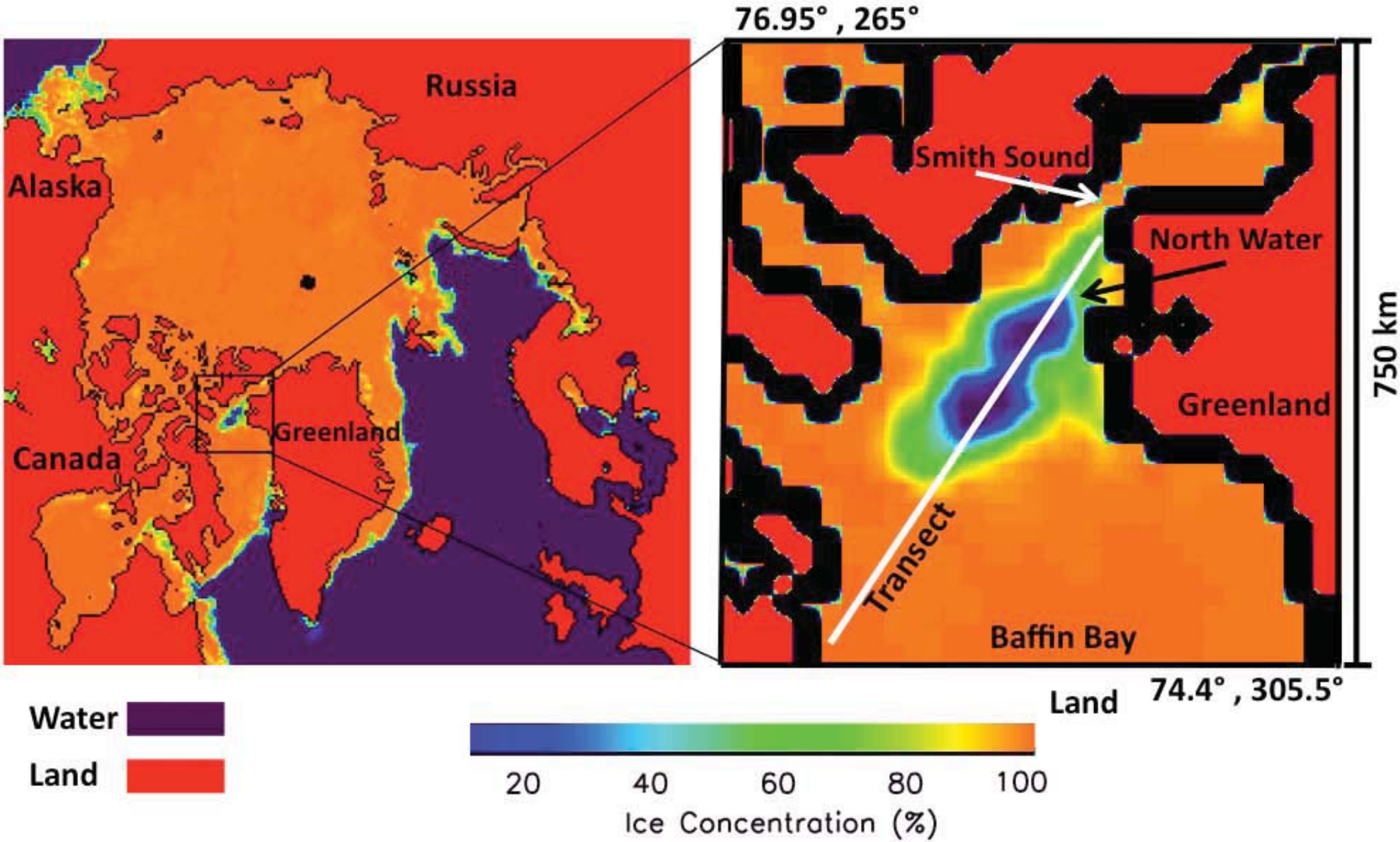
76.95° , 265°
Russia
Alaska
Canada
Greenland
Smith Sound
North Water
Greenland
Transect
Baffin Bay
750 km
74.4° , 305.5°
Water
Land
Land
20
40
60
80
100
Ice Concentration (%)

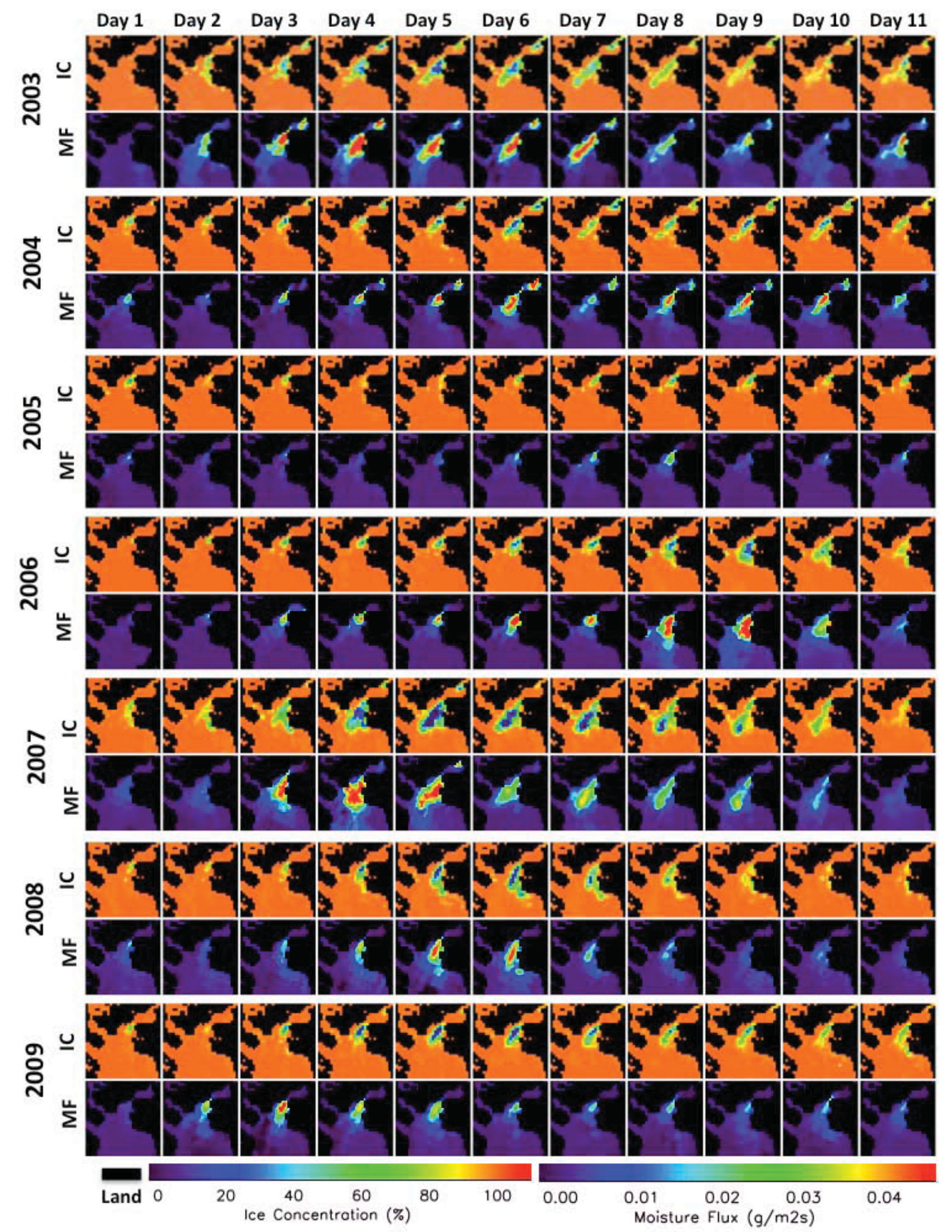
Day 1
Day 2
Day 3
Day 4
Day 5
Day 6
Day 7
Day 8
Day 9
Day 10
Day 11
2003
2004
2005
2006
2007
2008
2009
IC
MF
Land
0
20
40
60
80
100
Ice Concentration (%)
0.00
0.01
0.02
0.03
0.04
Moisture Flux (g/m2s)

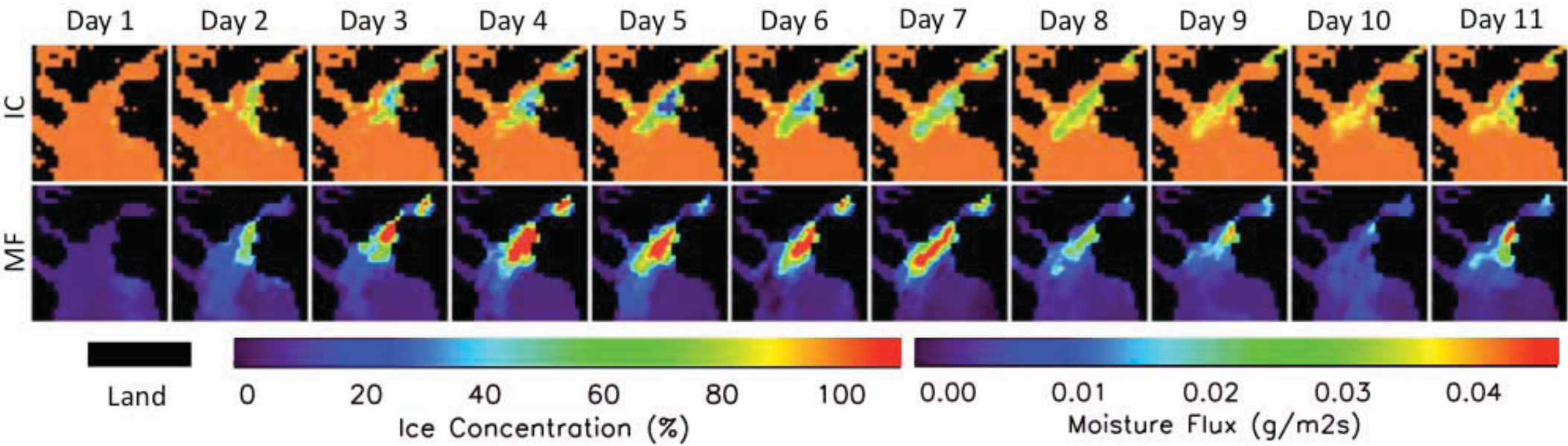
Day 1
Day 2
Day 3
Day 4
Day 5
Day 6
Day 7
Day 8
Day 9
Day 10
Day 11
IC
MF
Land
0
20
40
60
80
100
Ice Concentration (%)
0.00
0.01
0.02
0.03
0.04
Moisture Flux (g/m2s)

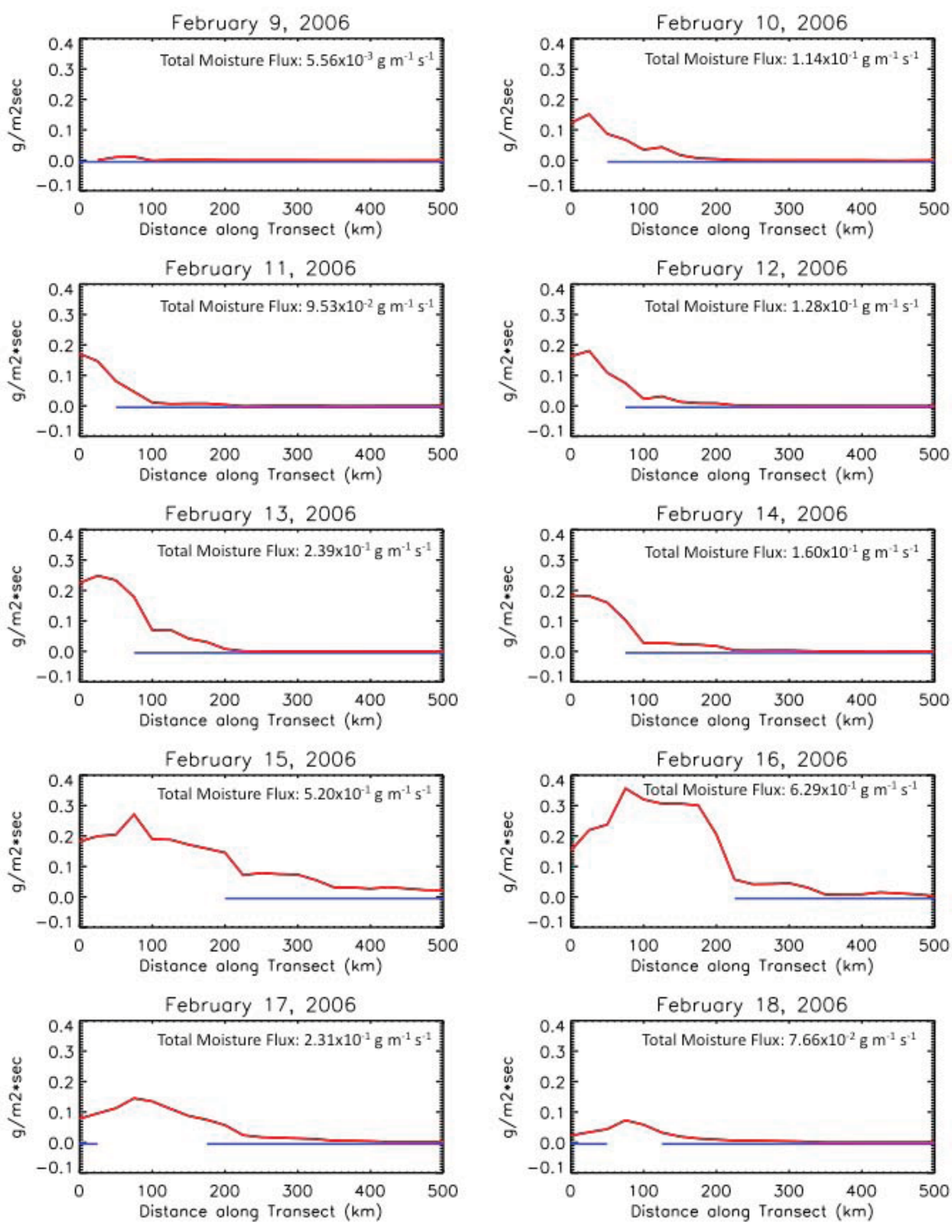
February 9, 2006
Total Moisture Flux: 5.56x10-3 g m-1 s-1
February 10, 2006
Total Moisture Flux: 1.14x10-1 g m-1 s-1
February 11, 2006
Total Moisture Flux: 9.53x10-2 g m-1 s-1
February 12, 2006
Total Moisture Flux: 1.28x10-1 g m-1 s-1
February 13, 2006
Total Moisture Flux: 2.39x10-1 g m-1 s-1
February 14, 2006
Total Moisture Flux: 1.60x10-1 g m-1 s-1
February 15, 2006
Total Moisture Flux: 5.20x10-1 g m-1 s-1
February 16, 2006
Total Moisture Flux: 6.29x10-1 g m-1 s-1
February 17, 2006
Total Moisture Flux: 2.31x10-1 g m-1 s-1
February 18, 2006
Total Moisture Flux: 7.66x10-2 g m-1 s-1
g/m2sec
g/m2•sec
0.4
0.3
0.2
0.1
0.0
−0.1
0
100
200
300
400
500
Distance along Transect (km)

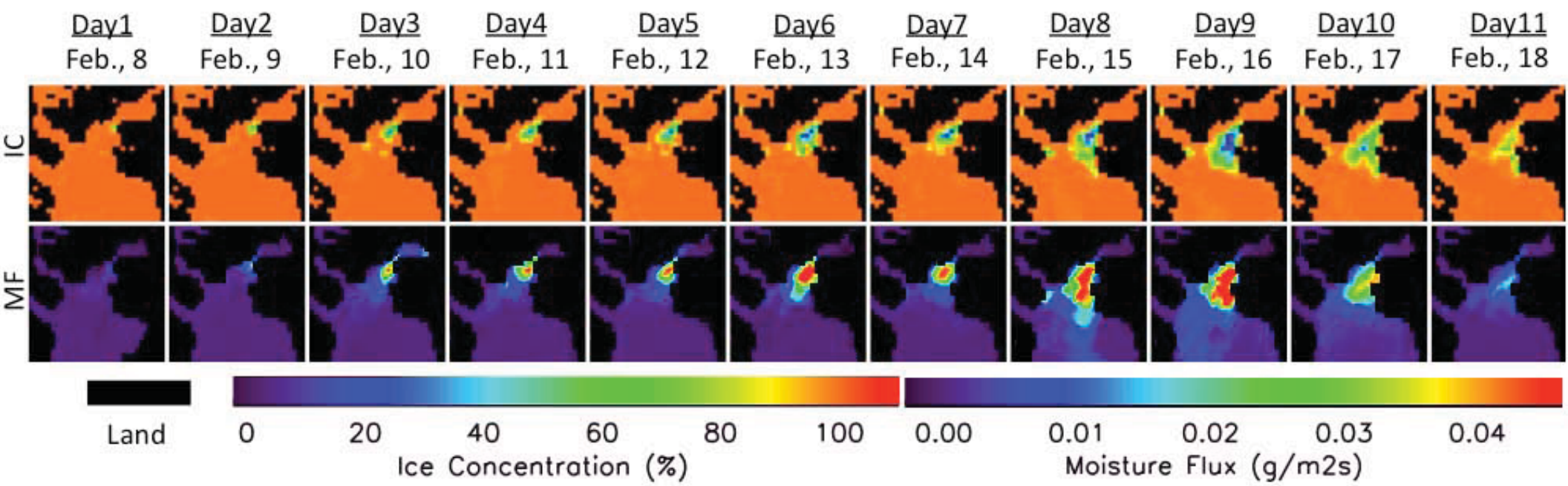
Day1
Feb., 8
Day2
Feb., 9
Day3
Feb., 10
Day4
Feb., 11
Day5
Feb., 12
Day6
Feb., 13
Day7
Feb., 14
Day8
Feb., 15
Day9
Feb., 16
Day10
Feb., 17
Day11
Feb., 18
IC
MF
Land
0
20
40
60
80
100
Ice Concentration (%)
0.00
0.01
0.02
0.03
0.04
Moisture Flux (g/m2s)

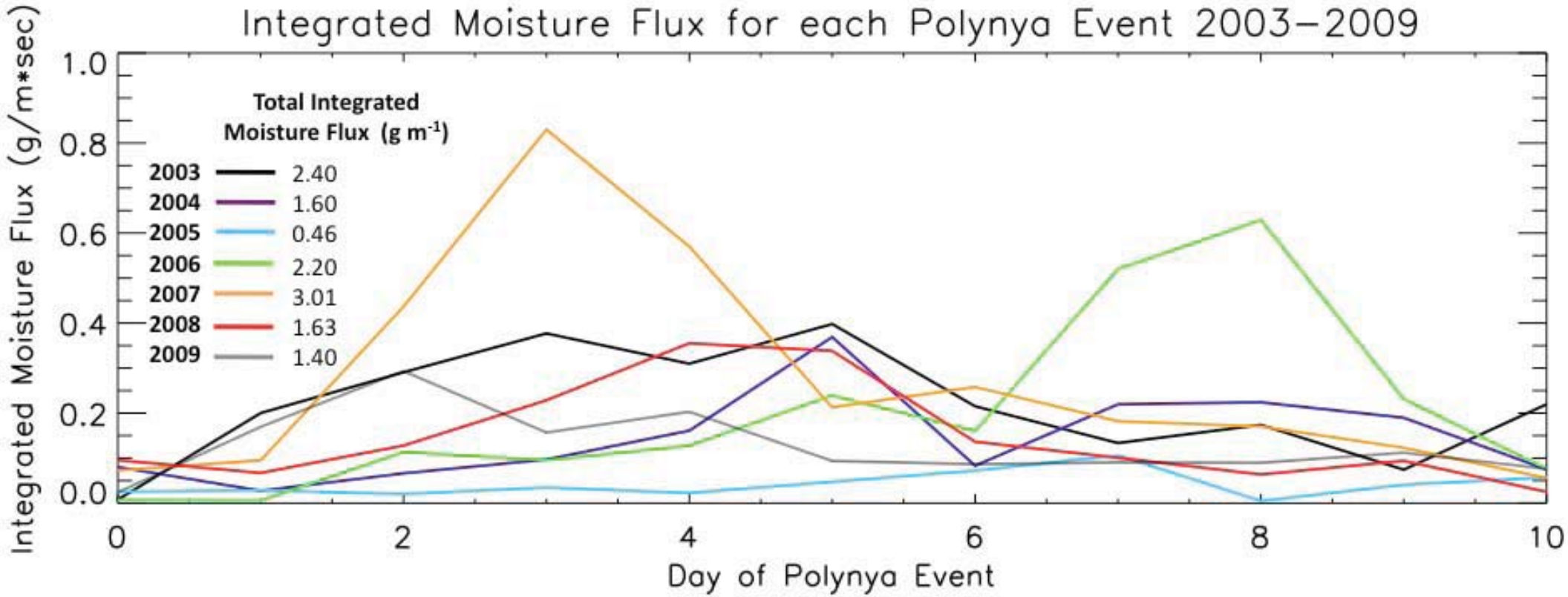
Integrated Moisture Flux for each Polynya Event 2003–2009
Integrated Moisture Flux (g/m*sec)
1.0
0.8
0.6
0.4
0.2
0.0
0
2
4
6
8
10
Day of Polynya Event
Total Integrated
Moisture Flux (g m-1)
2003 2.40
2004 1.60
2005 0.46
2006 2.20
2007 3.01
2008 1.63
2009 1.40

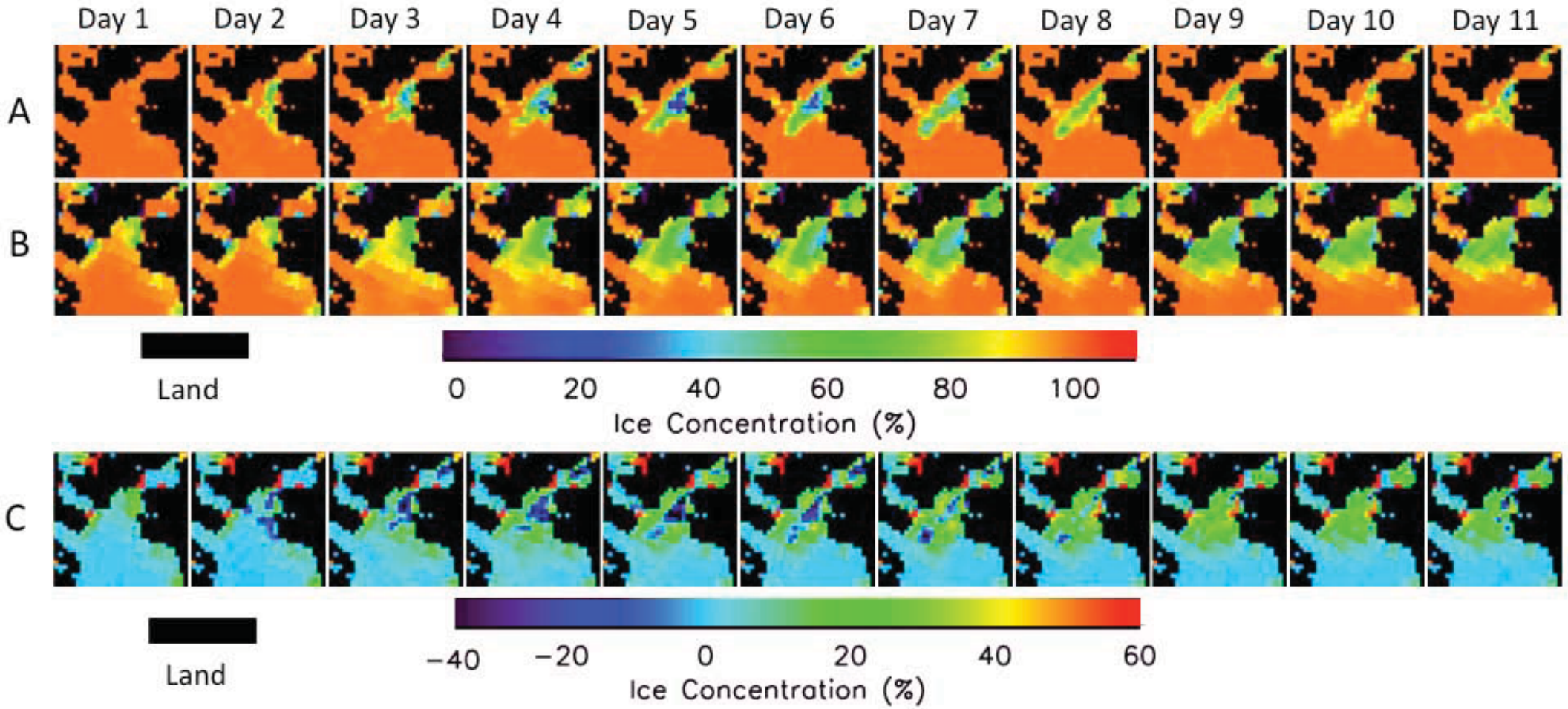
Day 1
Day 2
Day 3
Day 4
Day 5
Day 6
Day 7
Day 8
Day 9
Day 10
Day 11
A
B
Land
0
20
40
60
80
100
Ice Concentration (%)
C
Land
−40
−20
0
20
40
60
Ice Concentration (%)

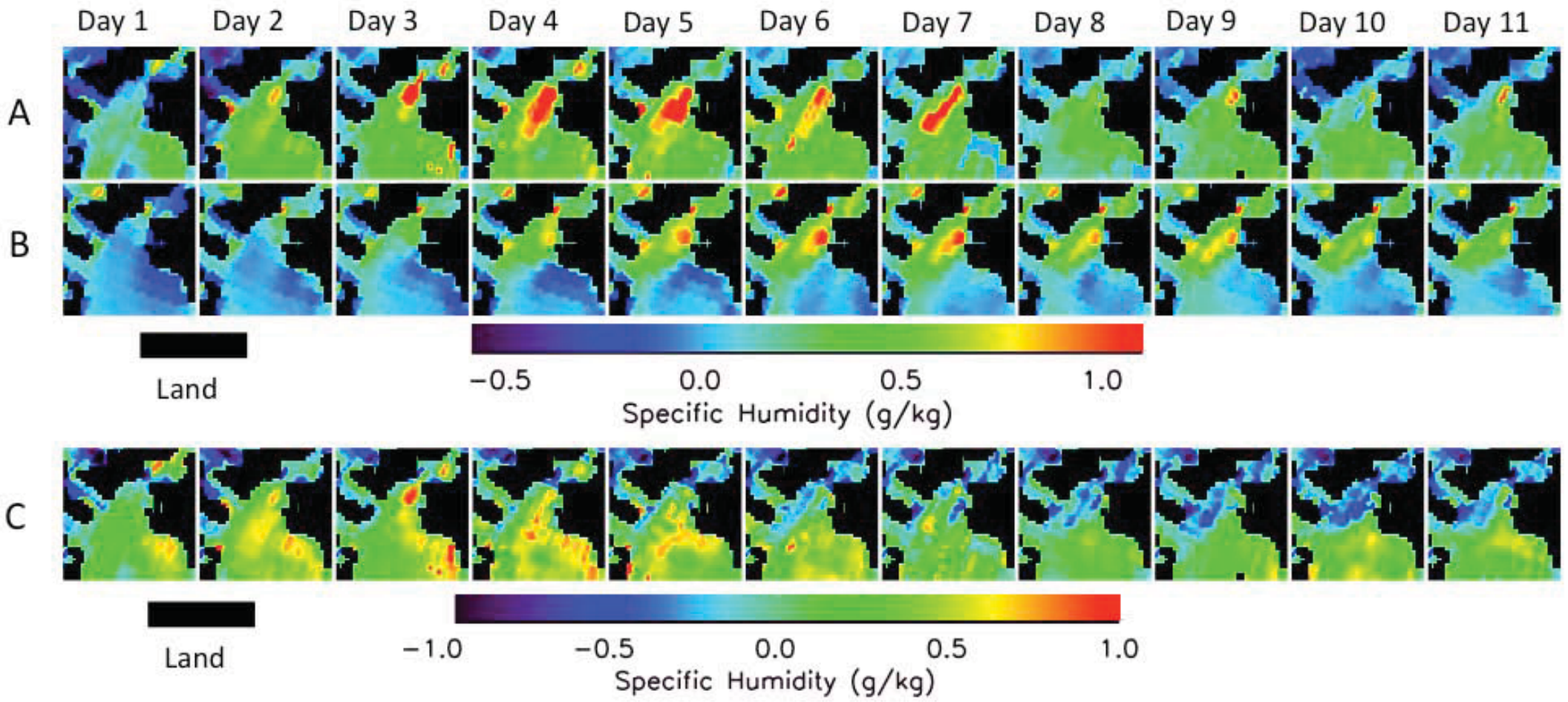
Day 1
Day 2
Day 3
Day 4
Day 5
Day 6
Day 7
Day 8
Day 9
Day 10
Day 11
A
B
Land
−0.5
0.0
0.5
1.0
Specific Humidity (g/kg)
C
Land
−1.0
−0.5
0.0
0.5
1.0
Specific Humidity (g/kg)

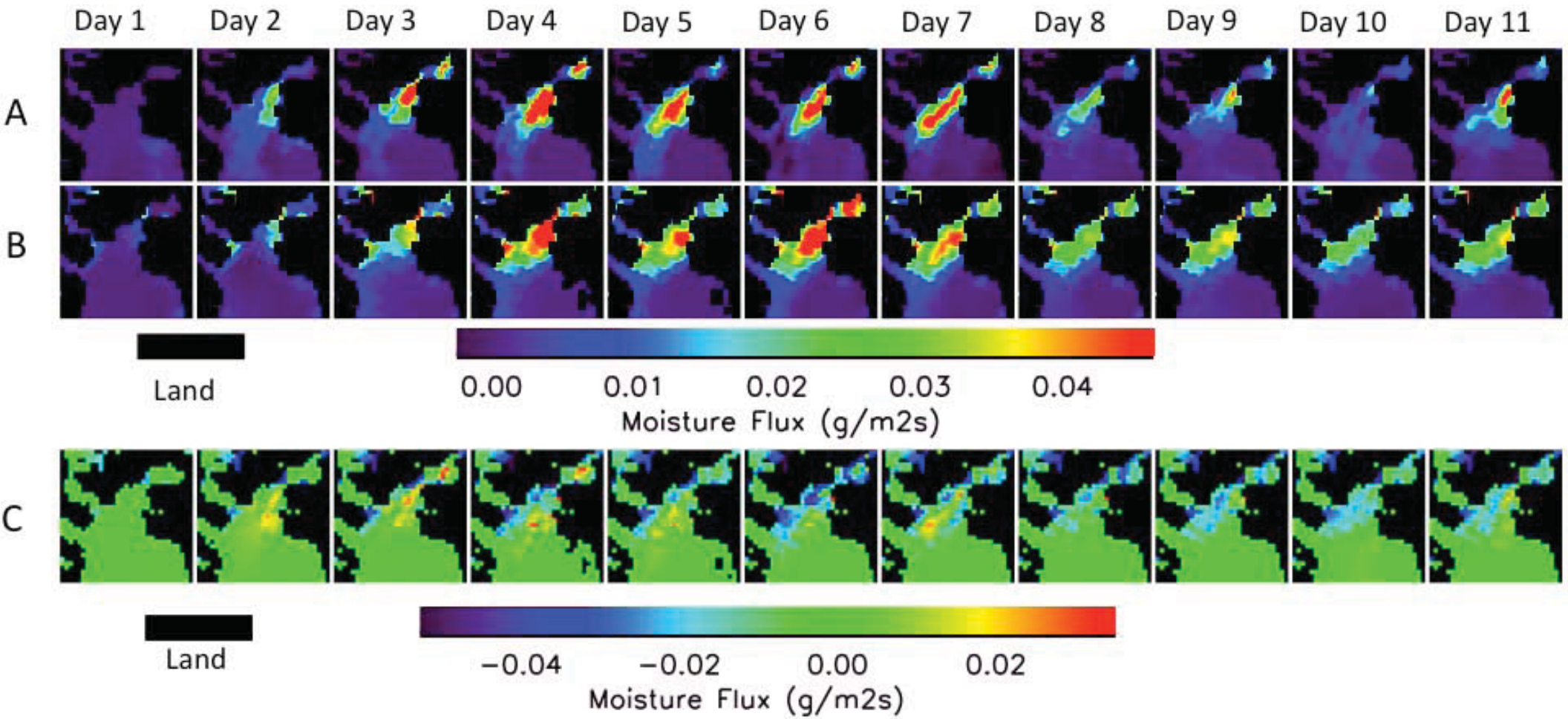
Day 1
Day 2
Day 3
Day 4
Day 5
Day 6
Day 7
Day 8
Day 9
Day 10
Day 11
A
B
Land
0.00
0.01
0.02
0.03
0.04
Moisture Flux (g/m2s)
C
Land
−0.04
−0.02
0.00
0.02
Moisture Flux (g/m2s)

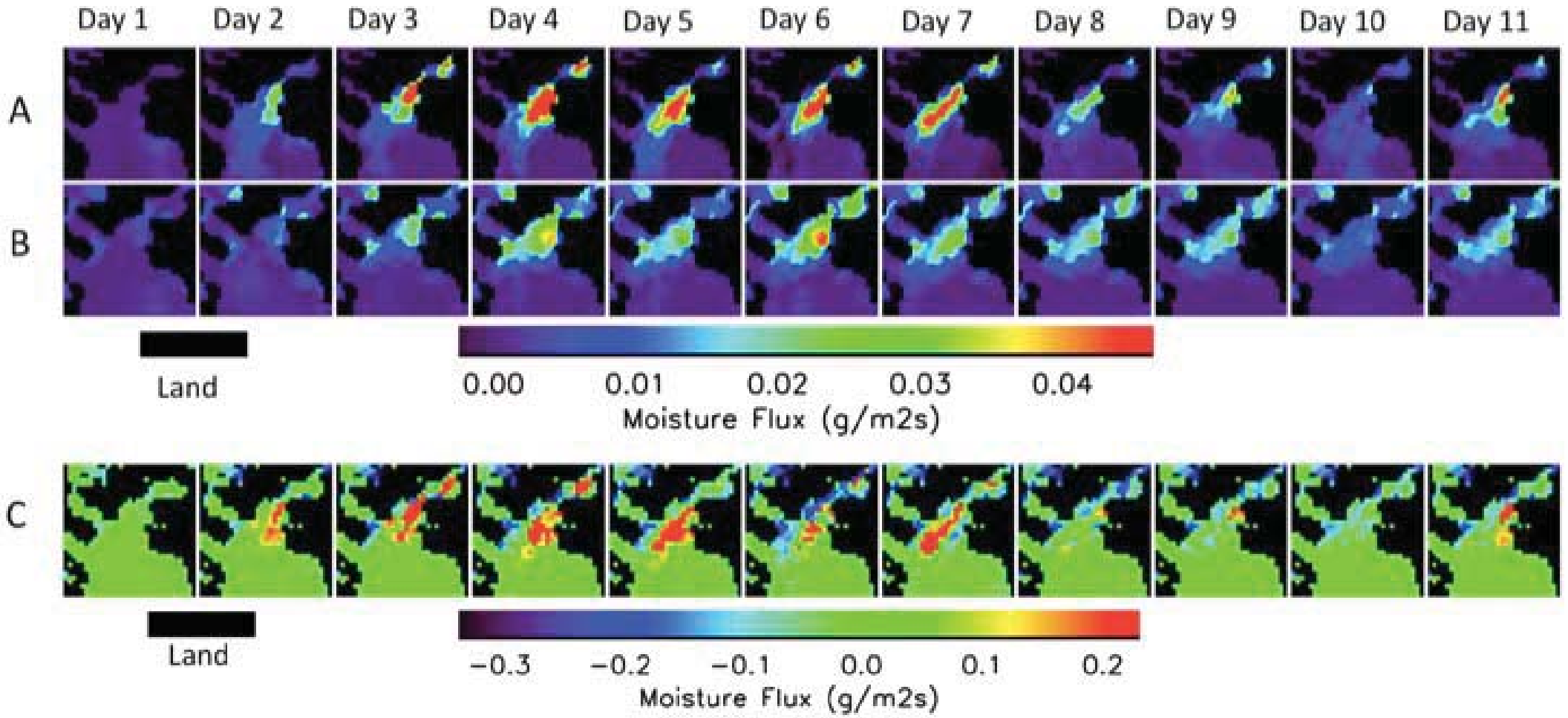
Day 1
Day 2
Day 3
Day 4
Day 5
Day 6
Day 7
Day 8
Day 9
Day 10
Day 11
A
B
Land
0.00
0.01
0.02
0.03
0.04
Moisture Flux (g/m2s)
C
Land
−0.3
−0.2
−0.1
0.0
0.1
0.2
Moisture Flux (g/m2s)